Mound Configurations on the Martian Cydonia Plain

Horace W. Crater

The University of Tennessee Space Institute
B. H. Goethert Parkway
Tullahoma, TN 37388-8897

Stanley V. McDaniel

Sonoma State University
1055 W. College Ave #273
Santa Rosa, CA 95401

Abstract — We show that a group of mound-like formations in the Cydonia area of Mars of relatively small and nearly uniform size have relative positions that repeatedly display symmetries in the apparent form of related right and isosceles triangles. We also show that these pairs cluster sharply in density about a certain value of the defining angle of those related triangles and that on average the vertices of the triangles lie significantly closer to the measured centers of the mounds than those for fictitious mounds from a computer simulation. Our computer simulation of the surrounding features and the mound formations themselves demonstrates that the numerous examples of these symmetries, the resultant clustering about certain proportions, and the relative precision of the vertices to the mound centers are not compatible with random geological forces. We have thus uncovered an anomaly of number, geometry, and precision. In order to give a quantitative measure of this anomalous distribution of mounds we determine the likelihood that we will make an error by rejecting the null hypothesis. This level of significance we find for our test is $p \sim 15.5 \times 10^{-6}$. That is, in a million trials, the repetition of the frequency of appearance of these triangles, greater than or equal to the observed (19) in the actual data, and with the observed or greater precision, is about 15 ± 2.5. In this computer simulation the average number of appearances is about 6, with a standard deviation of about 2. In 95% of the computer simulations, the distance of the vertices of the triangles was, on average, further from the (fictitious) mound centers than for the case of the actual mounds.

Keywords: Mars — Cydonia — mounds

Introduction

During the 1976 Viking missions to Mars, several images (primarily NASA Viking frames 35A72, 70A11, 70A13, and 561A25), taken over the area known as the Cydonia Plain, revealed some unusual surface formations. Over the intervening two decades, various independent researchers have studied

these formations, and have come to the consensus that the area exhibits a degree of anomaly sufficient to warrant active investigation of the site by future space probes (DiPietro *et al.,* 1982, 1988, 1990; Pozos, 1986; Torun, 1988, 1989; O'Leary, 1990; Carlotto, 1988, 1990, 1991, 1997; McDaniel, 1994; Crater, 1994, 1995, 1998, 1999; Erjavec, 1995).

Work by these researchers has focused primarily on several larger objects in the area (averaging about 1 km^2 in size). In 1994, Crater undertook to investigate the visually apparent geometric relationships found within a group of much smaller, hill-like features (mounds) located in the same vicinity (Crater, 1994, 1995, 1998, 1999). The area where the mounds are located is near the controversial "Face" formation. Our analysis of the apparently anomalous character of the mound distribution is independent of questions regarding the formation of the "Face." Although exact knowledge of the morphology of these objects must await higher resolution images, the Viking images are of sufficient resolution to make feasible a quantitative study of their spatial relationships, from which certain reasonably secure conclusions may be drawn.

Subject Matter and Hypothesis

The "small mounds" are a group of objects 0.1–0.2 km^2 in size located in the region of Cydonia under study. Approximately 16 objects in the area fall into this category. Figures 1 and 2 are for descriptive purposes and should not be used for measurement. In these small images, some highlights may be mistaken for "mounds" but are actually bright spots on larger features.

For the sake of clarity in identifying the mounds and their relative placements, the background is darkened in Figure 2 and the mounds have been brightened. Letter designations are also shown for 12 of the 16, excepting only
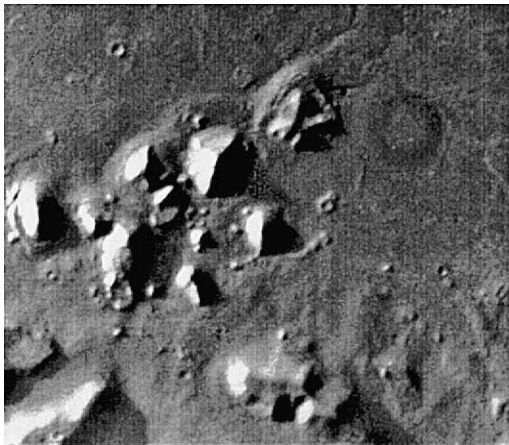
Fig. 1. A Portion of Viking Frame 35A72.
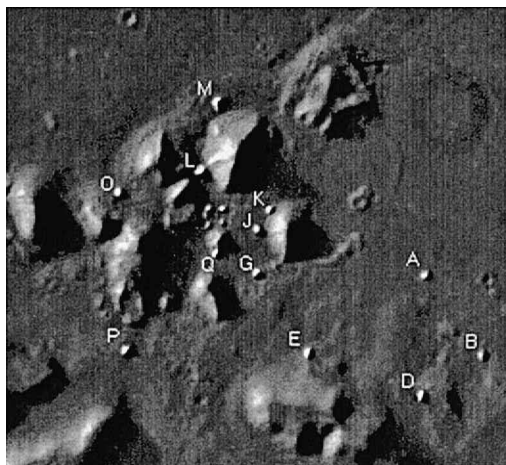
Fig. 2. Letter designations for 12 mounds.

four that are tightly clustered in the left center area of the image, where the letters would be too crowded. These four are discussed later on (in Section 5.A).

These objects are not tightly clustered but are separated in some cases by as much as 3 km. They are clearly distinguished from other land forms in the area not only by their size in relation to the larger surrounding features whose geological nature is evident (craters, mesas, and mountain-like features) but also by their brightness, which causes them to stand out from the general background. (In all figures except Figure 2, no features are electronically enhanced relative to the overall image.) Although the 47-m/pixel resolution is insufficient to reveal their fine structure, in the best image enhancements some of the mounds appear to cast a distinct shadow that comes to a point. They may be what geologists call sand boils, pugs, or perhaps dreikanters (three-sided pyramidal shapes resulting from wind erosion). Their exact intrinsic nature is not immediately relevant to this discussion.

There are several objects in Figure 1 (other than the ones lettered in Figure 2), that are either (a) significantly larger, (b) parts of larger structures obscured by shadows, (c) not clearly distinguished from other structures that they appear attached to, (d) have significantly reduced albedo relative to other mound-sized forms, or (e) associated with small pedestal craters.

Attention was first drawn to these objects because of the apparent regularity of arrangement among the six that lie in the relatively open area south of the larger formations, comprising mounds P, G, E, A, D, and B (see Figure 3). Specifically, within the margin of error for measurement and visually obvious, (1) triangle EAD is an isosceles triangle; (2) lines drawn from the estimated centers of mounds PG, EA, and DB are parallel; (3) lines drawn for mounds PE and GA are also parallel, forming a parallelogram PGEA; and (4) triangles drawn for mounds PGE and GEA are right triangles containing the same angles
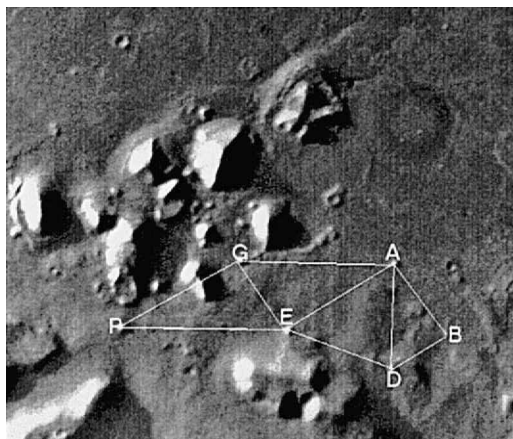
Fig. 3. Visually evident parallel lines, right and isosceles triangles.

and of the same size. Not as obvious visually but clear enough upon measurement, (5) triangles drawn for mounds GAD and ABD are again right triangles containing the same angles as PGE and GEA although different in size while the right triangle EAB has the same angles and same size; and (6) the isosceles triangle EAD has angles such that if it were bisected at the vertex at mound D, then it would be split into two right triangles that closely match the right triangle ADB, in both angles and size. These visually detectable relationships are shown in Figure 3 (detailed discussion of measurements in order of discovery to follow later). The visible regularities and the relative isolation of the six mounds involved warrant a more detailed investigation of the geometric characteristics of the mound configuration.

Methodological Considerations

Investigation of the geometric relationships between these mounds takes the form of a test of what may be called the *random geology hypothesis.* This hypothesis presupposes that the distribution of the mounds in the specified vicinity (*i.e.,* the area of other recognized anomalous formations), however orderly it may seem, is consistent with the action of random geological forces. Our question is: *Does the random geology hypothesis succeed or fail in the case of the small mound configuration at Cydonia?*

The random placement of a number of mounds may result in any number of orderly arrangements, seemingly unlikely to occur by chance. The probability, though small, that any one such arrangement is a result of random forces is not very meaningful. There may be many equally orderly arrangements that also may seem intuitively unlikely. For example, in the case of an arrangement of three mounds in the form of an isolated isosceles triangle, the probability of

that particular isosceles triangle occurring by chance is not as meaningful as is the probability of any isosceles triangle occurring by chance.

On the other hand, if a relatively simple pattern, precise within reasonable limits, occurs with unusual redundancy, then it becomes meaningful to focus *a priori* on that particular pattern. In our visual inspection of six mounds (GAB-DEP), we found evidence of an initial redundancy in the form of a series of similar right triangles each of which appears to be related to the isosceles triangle ADE (as described above, bisecting the isosceles produces two equal right triangles geometrically similar to the right triangle outlined by the mounds in the figure). This observed redundancy of associated right and isosceles triangles may well be a result of random placement. To test whether this is the case, we determine by computer simulation the odds that the number of appearances of these triangles will be greater than or equal to that observed. Due to the finite size of the mounds and the many triangles that can be drawn between vertices chosen from a multi-mound configuration, numerous appearances could very well be compatible with a random distribution. Under the random geology hypothesis we would expect odds on the order of 1 in 100 or greater. This is a common value for the level of significance used in statistical tests. It means that we reject the null hypothesis (our random geology hypothesis) if those odds are less than 1 in 100. The level of significance we find in this paper is $(15.5 \pm 2.5) \times 10^{-6}$. Technically this gives us the fraction of the time we would commit an "error of the first kind." This is defined as the error one makes by rejecting the null hypothesis when in fact it is true (Brownlee, 1965).

In Section 1 we present a detailed description of our criteria for selection of the mounds and tabulate their positions and sizes. For comparison we also give the size range of the larger features near the mounds. In Section 2 we describe the primary features of their apparently symmetrical arrangement, namely repeated appearances of similar isosceles and right triangles. We discuss the nature of the relations discovered and describe our methodology for testing the random geology hypothesis in Section 3, including a display of the results in graphical form. In Section 4 we determine the level of significance of our test and in Section 5 we describe further tests.

1. Selection Criteria for Mound-Like Land Forms

To those unfamiliar or only casually familiar with the Viking images, it may appear as though our selection of the "mounds" is arbitrary among a field of many possibilities. The reference images accompanying this paper do not show the detail that high-quality ortho-rectified enhancements display. (Orthorectification corrects for the distortion of angular placements of surface features in the image due to a non-overhead camera viewing angle.) Intimate familiarity with research quality images, however, reveals quite a different picture. There is a fairly obvious, clear-cut distinction between the "mounds" and the much larger structures in the area. In this section we present our selection criteria for the formations we have designated with the generic term "mound."

Measurements given below are obtained from ortho-rectified digital images processed from the original Viking data by Dr. Mark J. Carlotto and Mr. Erol Torun, both highly qualified professionals in image processing and cartography, respectively. Serious research requires reference to these enhancements or enhancements of equal quality. (The authors would welcome replication of their work and will provide orthographically rectified, research-quality images upon request.)

A. Size and Uniformity

The size of the mounds is noticeably smaller than the large structures in the area. The mounds are more or less uniform in size and general shape, with an average area of 76 square pixels, or about 0.167 km^2. In contrast, the larger features in the area are on the order of 1 km^2 or greater. The estimated areas (in km^2) of the 12 lettered mounds are given in Table 1. We estimated the areas by counting the number of times the X and Y counters on our imaging software changed values as we guided the pointer from one extreme side to the other. Using 47 m/pixel, we obtain the areas listed in the table. The uncertainties are on the order of 0.01 km^2. For comparison, the average area of the larger objects is about 1438 square pixels (about 3.16 km^2), with the largest being 4425 square pixels and only three being less than 700 square pixels (at 490, 400, and 225 square pixels). The smallest of the larger objects is nearly double the largest mound size. We also list in the table the relative location of all the mounds relative to mound G. Mound G itself is located at approximately 40.9° north latitude and 9.8° west longitude.

B. Albedo

Unlike some of the small hill-like features of similar size (for example the three or four formations in the area bound by mounds A, B, D and the two formations between E and P), the mounds we choose appear to have a high albe-

TABLE 1
Areas and Relative Positions of Mounds

Mound	Area in km^2	N/S from G in km	E/W from G in km
G	0.18	0.0	0.0
A	0.13	−0.05	4.8
D	0.14	−3.5	4.7
E	0.15	−2.3	1.5
B	0.12	2.3	6.4
P	0.18	−2.2	−3.7
K	0.16	1.8	4.2
J	0.15	1.2	4.7
L	0.22	2.9	−1.5
M	0.29	4.9	−0.9
Q	0.11	0.6	−1.1
O	0.22	2.3	−3.8

do. It is the relatively uniform brightness and similar size of the mounds that causes them to stand out noticeably against the background. On average the mounds are about 90% as bright as the brightest areas on the larger formations, and about 125% as bright as the mean background brightness. The sun angle in Figure 1 (Viking frame 35A72) is about 10°. In the other Viking frame (70A11), the angle is about 27°. In both cases, the surfaces of those mounds on the sun-facing side have this albedo display.

C. Shape

In most cases, the shadows of these formations taper to a point. This latter feature is especially noticeable in mounds A, B, D, E, P, L, and Q (see Figure 1). On mounds G and A, in the best enhancements, there are clearly visible surfaces indicating a faceted structure. Most other mounds display some evidence of triangular sides. Although mound O looks to be more rounded and does not appear to have such sharp features, a further examination of it from Viking frame 70A11 reveals angular surface features like the other mounds. We emphasize, however, that the shape is not the focus of this study.

D. Isolation

There are a number of features with significant albedo which at first sight look like mounds, but on closer inspection are found to be projections on larger structures. For example, this is true for four or five items found just above mound P. Three of these directly above mound P in Figure 2 are actually protrusions on a much larger formation. The rightmost of the five (at about 2:00 from P) looks like an isolated mound in Figure 1 (Viking frame 35A72) but is seen in frame 70A11 to be the illuminated peak of a protrusion extending from that larger formation. The leftmost (at about 11:00 from P) is eliminated because it has significantly reduced albedo relative to the other mound-size forms (it is not sun blocked).The mound-like structure to the far left center of the image is also a protrusion on a larger formation. In contrast to these, mound Q is very near a larger formation but is clearly separated from it. The same can be said for mounds L and M.

There is a close doublet formation about two thirds of the way up on the left portion of the figure, out on the open plain. We leave this out because it lacks albedo and its doublet structure makes its position ambiguous. We also leave out the twin mound-like forms that terminate a chain-like feature extending out to the east of the large oval structure adjacent to mounds K and J. These are clearly part of the chain and have a significantly lower albedo. Similarly a few low, rounded hill-like features near mound B do not have the same sharpness or albedo as B and so they are eliminated. We also eliminate from our candidates structures that appear to have clearly defined causative factors such as obvious association with a pedestal crater (there are several such cases).

Attention has frequently been drawn to the four apparent mounds located

roughly in the center of the larger structures and just to the left of mounds J and K. These four objects are arranged in a fairly regular pattern forming a cross, with an indication of a fifth, smaller mound-like feature at the center of the cross. (Actually the northernmost of these objects does not strictly qualify as a mound by our definition, as on closer inspection it appears to be elongated, generally rectangular, and in the shape of an open "L"). We do not include these four objects separately because the distances between them is on the order of their sizes, rendering angular measurements between them meaning-less. We will, however, treat them as a group later in this study.

2. Geometric Measurements

It was noticed early on that mounds E, A, and D appear to form an isosceles triangle (Hoagland, 1992). This isosceles can be clearly discerned in Figure 3. The obvious visual symmetry is rather striking. To confirm this early impres-sion, Crater made careful measurements. Since the mounds, though relatively quite small, are not geometric points, their angular relationships and the dis-tances between them were measured initially from their centers estimated within a determined margin of error.

First the X and Y coordinates of the approximate centers of the mounds and their uncertainties were determined using an ortho-rectified image (one that takes into account camera angle). In the electronic imaging software (Photofinish), those coordinates appear as a pair of integer digits that change in whole units as the mouse pointer is moved over the image. Each unit is re-ferred to as a "pixel." X and Y coordinates were also obtained by direct mea-surement on hard copy. Three different ortho-rectified images based on two different Viking frames (35A72 and 70A11) were used to cross-confirm mea-surements. (The recent images taken by the Mars Global Surveyor displayed only a very few of the mounds and were not used in our analysis). The angle measurements presented here are from 35A72. Although the mounds are nei-ther perfect circles nor squares, it is possible to locate their (approximate) geo-metric centers. The X and Y coordinates were recorded when the pointer was nearest this location. The uncertainty was normally one or two pixels either way based on numerous re-measurements. The mound sizes in the same units was 3–6 in either direction.

Then by means of the Pythagorean theorem and the law of cosines, triangle EAD, as measured from those initial reference points, was found to contain the following angles: $71.1° \pm 3.2°$, $55.6° \pm 2.9°$, $53.2° \pm 2.7°$. Averaging the last two figures, this measurement is very close to an isosceles triangle of $71°$, $54.5°$, $54.5°$ which would fall well within the measurement error for the mound cen-ters.

It had also been noticed by earlier investigators (Hoagland, 1992) that the triangle formed by mounds E, A, and G is a visually obvious right triangle. The base of the isosceles forms one side of this triangle (Figure 4). Measurements from the apparent mound centers yield $88.7° \pm 3.9°$, $35.0° \pm 1.9°$, $56.3° \pm 2.8°$.
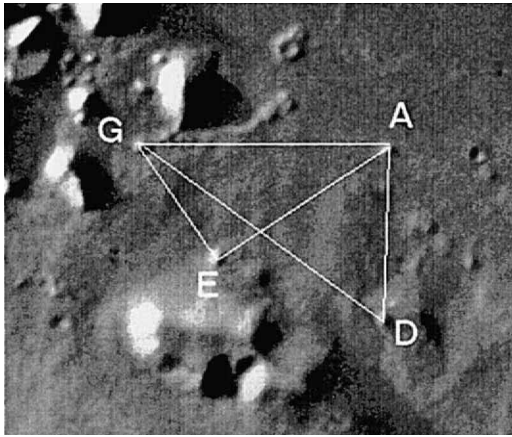
Fig. 4. Two similar right triangles.

Furthermore there is another visually apparent right triangle, with vertices GAD. Its angles work out to be $88.2° \pm 2.70°$, $36.6° \pm 1.7°$, $55.2° \pm 2.4°$.

There are two remarkable features about these two right triangles. The first is that within the accuracy of the angular measurement, which averages about $2.5°$, the two right triangles (GAD, EAG) appear to have the same angles. The second is that these two apparently similar right triangles have angles that are consistent with one that bisects the isosceles triangle shown in Figure 3. Such a bisection would produce right triangles with angles of approximately $90°$, $35.5°$ and $54.5°$, consistent with the above right triangles (Figure 5).

A fifth mound (B) appears to form two other right triangles ABD and EAB (Figure 6). We find that triangles ABD and EAB contain respective angular measurements of $90.9° \pm 5.4°$, $52.6° \pm 3.3°$, $36.5° \pm 2.2°$ and $90.0° \pm 3.9°$, $55.2°$
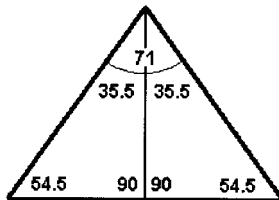
Fig. 5. The isosceles and right triangles appear to be related.
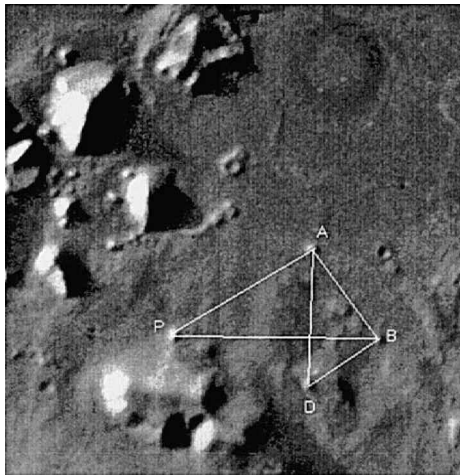
Fig. 6. Two more similar right triangles.

± 2.4°, 34.8° ± 1.5°. Within the measuremental uncertainties they are both clearly similar to the two right triangles that appear in Figure 4. There appears now to be a trend in the data, suggesting a quasi-predictable phenomenon. If so then this trend should continue within the other mounds.

A sixth mound, P, to the west of the five mounds is a relatively isolated mound, yet we find that the triangle formed by mound P with mounds E and G (Figure 7) is again a candidate for a right triangle (angles 92.1° ± 3.8°, 32.1° + 1.8°, 55.8° ± 2.7°) of approximately the same angles as appears in the four right
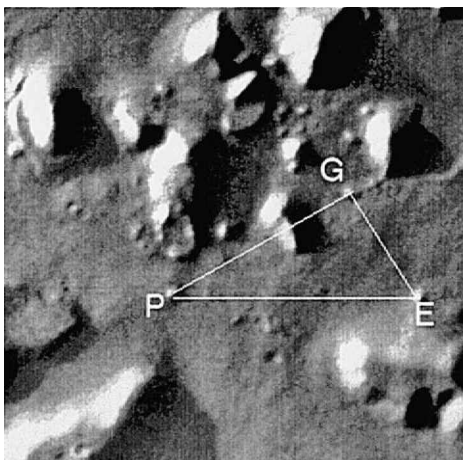
Fig. 7. Right triangle PGE, equal to AEG.

triangles that appear in Figures 4 and 6. Furthermore, it is "back to back" and equal in size, within the margin of error, to two of those right triangles GEA and EAB (see Figures. 3, 4 and 6).

Does this trend of redundancy include the isosceles as well as right triangles?

Including a seventh mound M (Figure 8) adds another larger version (PMA) of the isosceles triangle ADE of Figure 3 with angles of 55.1º, 54.7º, and 70.3º with similar uncertainties as before. Note that this triangle shares vertex A in common with the other isosceles ADE.

By empirical determination, following the clue provided by the visually obvious regularities, we have found an evident redundancy in the appearance of specifically related isosceles and right triangles within a calculated margin of error. As we shall discuss in Section 3C, this redundancy appears to extend to the mounds to the north of the initial six mounds displayed in Figure 3. Is the mound distribution, despite these redundancies, consistent with the random geology hypothesis?

3. Statistical Analysis of the Mound Geometry

A legitimate criticism is that we have not accounted for the role of numerous other combinations among the mounds. (There are 220 triangles altogether defined by the 12 mounds). Nor has the above exploratory analysis taken into account other classes of right and isosceles triangles. We meet these objections by examining the set of *all* right and associated isosceles triangles, not just the ones encountered above. Furthermore, in order to account for the above-mentioned combinations we will devise a statistical test of the random geology hypothesis based on computer simulations. In this section, these examinations and tests show decisively that these pairs of related right and isosceles triangles
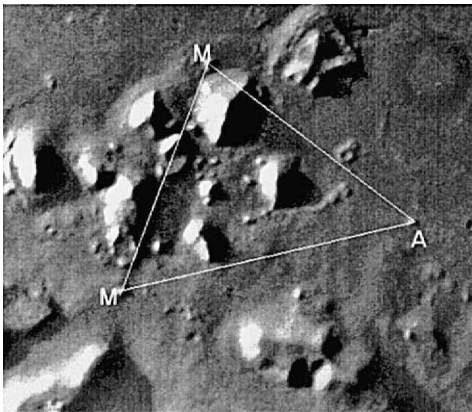
Fig. 8. Isosceles PMA, similar to ADE.

cluster sharply about a certain defining angle and that this peak is high above random expectations.

A. Mound Placement Analysis

The triangles found in our exploratory analysis above have a connection which we may quantify by defining their angles with one parameter which we will call t. In terms of this parameter, the angles of an arbitrary right triangle can be written as simple linear functions of t and π with angles (in radians) defined by $\pi/2$, $(\pi/4 + t/2)$, $(\pi/4 - t/2)$. (In degrees, 90°, 45°+ $t/2$, 45°− $t/2$.) The partnered isosceles would then have angles defined by $(\pi/2 - t)$, $(\pi/4 + t/2)$, $(\pi/4 + t/2)$. In degrees, $(90° - t)$, $(45° + t/2)$, $(45° + t/2)$. We then perform our analysis according to the following prescription:

(A.1) We allow t to vary from 0° to 90° in 0.5° steps. Thus, defining $t = (n-1)/2$ we start with $n = 1$, in which case $t = 0°$. In this initial case the isosceles and right triangles are equivalent (both are 45° right triangles, *i.e.,* 90°, 45°, 45°).

(A.2) At each step, using a computer program, we determine the angles in all possible triangles (220 altogether) that can be drawn between vertices located at the centers of each of the 12 mounds. From these, the program then identifies candidate right and isosceles triangles, ones with angles within a reasonable prescribed limit of the ideal right and isosceles triangles described above for a given value of t. Once they are identified, we then vary the X and Y coordinates of the common vertices of the candidate triangles away from the center but within the areas of the mounds to see if a fit to the actual ideals can be achieved within a preset precision (done here for two values, 5° and 0.2°). This variation is continued until one achieves a *coordinated fit* to the ideal triangles, with all of the angles agreeing within less than the preset precision level. This is accomplished using a least-squares fitting routine. As this variation proceeds, some candidates drop out while on occasion some originally not identified candidates may appear. The process continues until the maximum possible number of right triangles and associated isosceles triangles (with angles defined as above in terms of t) have been fit within the precision level indicated.

A *coordinated fit* requires that *the same vertex within any given mound is used for all the triangles having one vertex sharing that mound,* not shifted about arbitrarily within each mound to accommodate each triangle separately. As an example of what this means we refer to Figure 3 which represents a six mound coordinated fit involving similar right triangles and related isosceles triangles. This stringent requirement for a coordinated fit severely restricts the number of chance matches. Note that the mound areas and placements could very well be such that the ideal for a given t would be impossible to fit, or very few triangles would achieve a coordinated fit.

Once this procedure, (A.1)–(A.2), is finished we record the number $(N(t))$ of those types of triangles achieving a coordinated fit for the given value of t. (For example, for $t = 10°$ the number of triangles achieving a coordinated fit within a 5° precision level is 15 triangles, or $(N(t)) = 15$.)

(A.3) The above two steps are repeated for $n = 2, ..., 181$ corresponding to $t = 0.5°$ to $t = 90°$ with $N(t)$ recorded at each step.

(A.4) The above analysis, (A.1)–(A.3), is repeated for both levels of precision (5° and 0.2°). The results are then plotted together with expected random distributions, as described below (see Figures 9 and 10).

B. Simulated Mound Placement Analysis

In order to test for the validity of the random geology hypothesis we make a computer simulation of randomly distributed fictitious mound locations. Since the designated region contains not only mounds, but ten much larger structures, we design a simulation containing both types of features, as follows:

(B.1) First ten large circular regions are distributed randomly by computer, using a random number generator, over an area comparable to the area in which the Cydonia mounds appear (about 67,000 square pixels) in such a way that they do not overlap. The areas of the fictitious larger features are chosen randomly to lie within the range of areas of the actual larger features. The individual areas of the ten larger structures are tabulated as follows (from greatest to least, in square pixels): 4425, 2350, 2040, 1950, 1040, 740, 720, 490, 400, and 225.

(B.2) Next, a set of 12 fictitious mound placements is generated also using a random number generator. Each set of fictitious mound center locations is thus randomly scattered over the chosen area such that, like the actual data, the mounds do not overlap with the larger structures nor with each other.

In both cases (B.1) and (B.2), the randomized data is constructed as follows:

(a) The random number generator provides two random numbers between 0 and 1. These are used to fix the X and Y coordinates, within an area one unit square, for the center of one of the fictitious mounds or large structures. This is repeated for each fictitious mound and larger structure.

(b) Second, this unit area and the center coordinates of the set of fictitious mounds and large structures are scaled so that the unit area becomes equal to the number of pixels of the general area in which the actual mounds are located (again, in the image this is about 67,000 square pixels, or about 148 km^2).

(c) The areas of the fictitious mounds, also in square pixels, are chosen randomly by computer from the range of areas of the actual Cydonia mounds just as the areas of the fictitious larger structures are constructed randomly from the range of areas of the actual large structures.

(B.3) Steps (A.1) and (A.2) that were taken for the actual mounds in the previous subsection are repeated here for the 12 fictitious mounds. A "hit" is recorded if and only if the vertices of the special right and related isosceles triangles contained in the model lie within the confines of the fictitious mound areas of a given fictitious mound configuration and the angles are within the preset limit of precision. The maximum number of hits is obtained by the same coordinated fit procedure (see (A.2)) used for the real mounds. Call this number $N_i(t)$, in which i labels the run number.

Note that this number $N_i(t)$ is sensitive to the size of the general area chosen to enclose our randomly generated mounds and large structures. As mentioned above, that area is chosen based on the actual image (see Figure 1). There is an *a priori* reason for concentrating on this region (as opposed to ones far outside the boundary). This is the primary region that includes the features that have been cited by other researchers as indicating possible anomalous structures. In other words we did not randomly select this area for study.

The area which includes those other structures is significantly greater than the portion of the image we have presented. However, this greater area has, relatively speaking, very few other mounds. If the area chosen both for our real data and the simulated data was taken to be that large, then the number of real mounds would not be substantially increased, on average the fictitious mound centers would be randomly placed further from each other, making the range of angles subtended by coordinated fits from mound to mound smaller. Thus the probability for obtaining fits to the ideal geometry would be artificially too low since this would make ideal pattern mismatches more likely. If the area chosen was significantly smaller than that shown by the image, this may also lower the probability by ignoring the increased odds if other real mounds could be included. The question of the area chosen represents the primary uncertainty in our analysis, but our choice is a conservative one. The area of 67,000 square pixels is a square area with a length of about 12 km on a side, and was chosen so that the perimeter includes all the mounds. Furthermore, we chose the perimeter as close, on average, to the outermost mounds as that expected on the basis of randomly distributed points within a fixed perimeter.

(B.4) Next we record for this value of t the value $N_i(t)$ for this randomly generated ith set of mounds.

(B.5) Repeat steps (B.2)–(B.4) a sufficient number of times (call it M) so that the average number, Equation (1), and the standard deviation, Equation (2), settle down to constant values.

$$\overline{N}(t) = \frac{1}{M} \sum_{i=1}^{M} N_i(t) \tag{1}$$

$$\sigma(t) = \sqrt{\frac{1}{M-1} \sum_{i=1}^{M} \left(N_i(t) - \overline{N}(t)\right)^2} \tag{2}$$

(B.6) Steps (B.1)–(B.5) are repeated for $n = 2, ..., 181$ corresponding to $t = 0.5°$ to $t = 90°$. As with the real mound analysis (A.4), two sets of precisions were used.

C. Discussion and Graphical Display of Results

Our question is: How many of these right and associated isosceles triangles occur in a coordinated fit among these 12 mounds, and what is the relation of that number of occurrences to chance distribution? Although there are 16 mounds in the area, as previously stated four of them are so close together in relation to their size that angular relations between them allow too much freedom for interpretation. We therefore restrict our procedure to 12 mounds, but take the four mounds into consideration later on.

To avoid possible bias toward any particular pair of right and isosceles triangles, or equivalently towards any particular angle t, we have examined the set of all right and associated isosceles triangles by allowing t to vary in $1/2°$ intervals from $0°$ to $90°$. The graphical display of the results of our tests is in the form of a distribution and allows us to determine if there is any clustering of the number of such triangles about any particular value of t.

The results are displayed in graphs for two different levels of precision. For a $5°$ precision we plot (for the actual mounds) the number $N(t)$ of coordinated fits of right and associated isosceles triangles having angles that agree with the ideal within less than $5°$. Then, for greater precision we plot $N(t)$ for triangles having angles that agree with the ideal within less than $0.2°$. For both degrees of precision we plot a comparison curve for the average number of triangles $\overline{N_i}(t)$ that should occur by chance. This comparison curve is obtained by the simulations described above.

(C.1) First Plot: $5°$ Precision (Figure 9). Figure 9 compares the plot for $N(t)$ with the plot for $\overline{N}(t)$ when the precision required for a coordinated fit among all 12 mounds is $5°$.

The plot in Figure 9 for the actual number of triangles for each value of t shows a broad rise and tapering off from about $6°$ to about $30°$. The plot for $\overline{N}(t)$ in the same figure shows a similar rise and tapering off. For both curves we find a distinct dip or decrease in the number of triangles when $t = 30°$. This dip reflects the fact that the isosceles triangles become equilateral for $t = 30°$
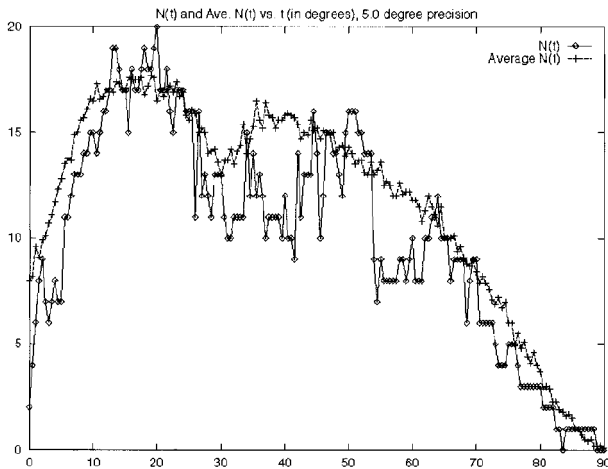
Fig. 9. $N(t)$ and $\bar{N}(t)$ *vs.* t (in degrees), 5.0 degree precision.

and triangles which are equilateral (or nearly so) are much less likely to occur by chance.

The two curves match reasonably well: At this level of precision there is no significant deviation from background and this result would tend to support the random geology hypothesis. We remind the reader that the coordinated fit points are not restricted to the centers of the mounds but are allowed to vary within the perimeters of the mounds (subject, however, to the constraint of a coordinated fit). With this lower precision, that variation stops when the angles of the candidate triangles match those of either the ideal right triangle or ideal isosceles triangle within less than 5°. When that coordinated fit variation continues until we achieve a higher precision, many candidate triangles fall by the wayside and if the Cydonia mound distribution was random it would likely fall along with the computer generated curve.

(C.2) Second Plot: 0.2° Precision (Figure 10). We find that when the precision is increased, a peak at $t = 19.5°$ emerges decisively from the background. (This is close to our estimate of 19° based on measurements of the initial mounds (see Figure 5)).[1] Figure 10 shows a well-defined peak of 19 occurrences at this angle (12 similar right and seven similar isosceles triangles), in the same region where a broad peak was seen in the lower precision plot. In our 12 mound coordinated fit, the six mounds K, J, L, Q, M, and O to the north of G, A, B, D, E, and P contribute seven additional copies JPD, PGL, GKL, AEL, PLA, MQA, GKQ of the right triangle similar to EAG, DAG, ABD, EAB, and

---

[1]Note: Because of the finite size of the mounds there is a range of nearby t values that give large N, but only one for $N=19$.
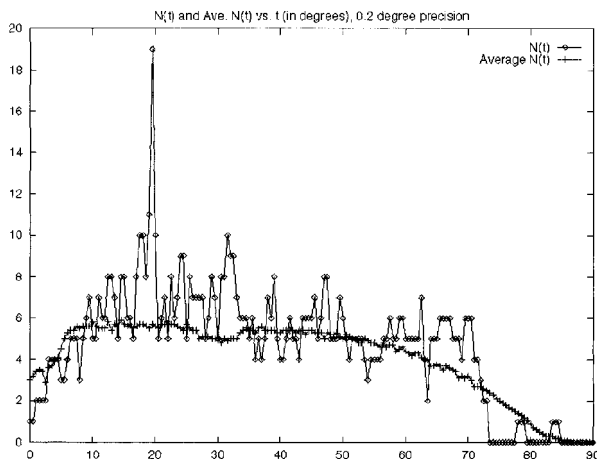
Fig. 10. $N(t)$ and $\bar{N}(t)$ *vs.* t (in degrees), 0.2 degree precision.

PGE seen earlier for 12 similar right triangles altogether. In addition, those remaining mounds K, J, L, Q, M, and O contribute five additional copies KAE, PEL, QJG, KLQ, and GMO of the isosceles triangle similar to those of PMA and ADE described in Figures 3 and 8, yielding seven isosceles triangles with the same proportions. Nineteen of these special right and isosceles triangles appear in our 12 mound *coordinated* fit (one vertex per mound restricted to the mound perimeter, not necessarily the center).

The comparison curve in the above plot for the $\bar{N}(t)$ random distribution retains the same general shape as it had for the lower precision, but as expected, drops dramatically in scale, with its high plateau now reaching only as high as six occurrences as a result of the greater precision required. Any further increase in the precision to still smaller angle uncertainties would not change these plots significantly because of the finite mound size. The peak clearly indicates an anomaly. The actual mound distribution contains an inordinately high number (19) of related right and isosceles triangles when $t = 19.5°$. For a random distribution we would expect a graph more like Figure 9 where the signal is buried in the noise. At the precision level of 0.2°, we find that $\bar{N}(t) = 5.7$ and $\sigma = 2.0$)

4. Level of Significance — an Anomaly of Number and Precision

Following up on the sharply defined differentiation between those triangles where $t = 19.5°$ and those for all other values of t, Figure 11 summarizes the results of 10,000,000 simulations of the random placements of 12 fictitious mounds among the larger features. The distribution function $F(N)$ gives the number of times out of that total of 10,000,000 that there will be N appearances of the right and associated isosceles triangles for $t = 19.5°$. On the X axis
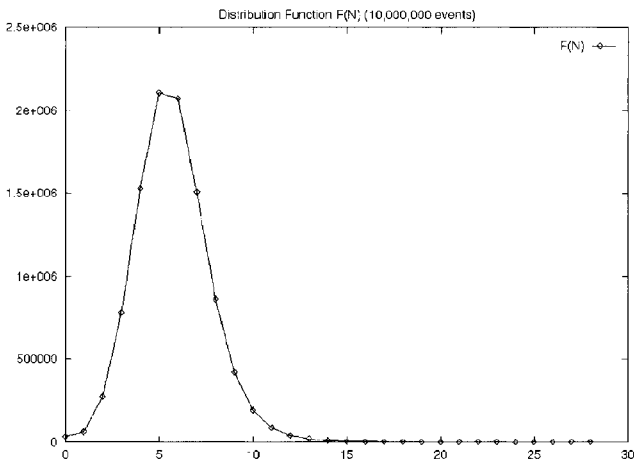
Fig. 11. The Distribution Function F(N) *vs.* N.

we have the number N of such triangles and on the Y axis the number $F(N)$ of random distributions of simulated mounds (computer runs) that produce that number N of triangles.

Looking at the curve $F(N)$ in Figure 11, we see a curve centered about a mean value $\bar{N}(t)$ of about 6 and width of about 2. In contrast to these figures for random distributions, the value of N corresponding to the actual Cydonia data (19) occurs far to the right where the curve tapers off, effectively outside the curve, just under 7 standard deviations away from the mean.

However, the distribution curve $F(N)$ is not a normal curve. This can be seen in the plot of Figure 12 of log($F(N)$) *vs.* N. If the distribution were normal then the log curve should be quadratic. Instead, for larger N we see a nearly linear curve. We speculate that the non-normal behavior occurs as N increases because the constraints imposed by geometry on a finite number of mounds enhance appearances of still more of the ideal triangles. Although we do not analyze the exact cause here, what this means is that we cannot estimate the probabilities of the actual frequency of 19 being the result of chance by extrapolating the complimentary error function (associated with a normal curve) out to 7. Thus, we are forced to take a more direct, though very time-consuming route. We computed directly the odds or level of significance of our result.

In order to obtain a more representative measure of the level of significance of our results we should take into account another important aspect of our coordinated fit, and that is the precision with which the coordinated fit points adhere to the center of the mounds. (The above two curves have no restriction on this measure.) It was noticed early in our research that the more visibly obvious symmetries, such as those represented in Figure 3, have the further remarkable feature that the fit points are very close to the center of the
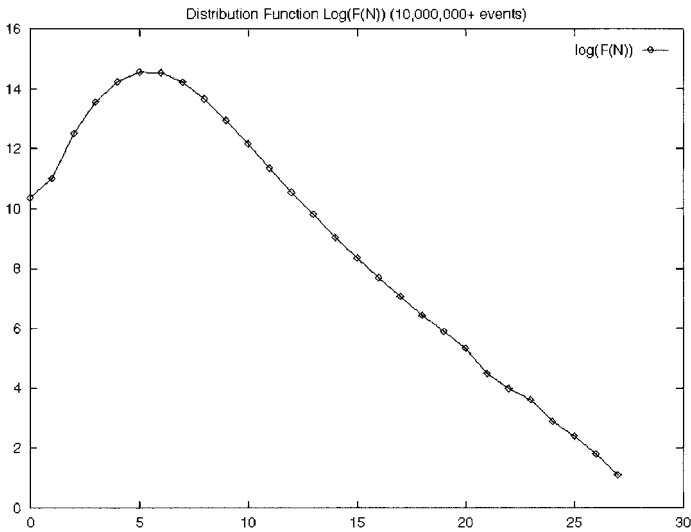
Fig. 12. The Distribution Function log(F(N)) *vs.* N.

mounds. Like the number of redundant right and isosceles triangles, this is also an anomaly relative to what one would expect, based on chance alone. We found that the average distance $\bar{d}$ of the coordinated fit point from the measured centers of each of the 12 actual Cydonia mounds is less than the corresponding distances on the randomly generated data in almost 95% of the ten sets of one million computer simulations. This $\bar{d}$ is defined as the summation shown below:

$$\bar{d} = \frac{1}{N} \sum_{i=1}^{N} \sqrt{\left(x_i - x_{i0}\right)^2 + \left(y_i - y_{i0}\right)^2} \qquad (3)$$

in which N is the number of mounds in the configuration (here there are 12 mounds); x_{i0}, y_{i0}, are the coordinates of the estimated center of the mound i; and x_i, y_i are the coordinated fit points within the mounds of the vertices of our desired triangles.

The $\bar{d}$ value gives a quantitative measure of how close, on average, the coordinated fit point within each mound is to the center of that mound. The smaller $\bar{d}$ is, the closer the coordinates of vertices of the ideal triangles lie to the approximate center of the mound. A $\bar{d}$ of 0.0 would indicate a fit in which all vertices were directly on the estimated mound center. The $\bar{d}$ needed for a precise fit (within 0.2°) of the model in the case of 19 triangles for the 12 mounds (in the case of $t = 19.5$) was 3.45 pixels. The larger majority of all computer simulated fits had $\bar{d} > 3.45$ pixels.

We need a measure of the level of significance that accounts for both anomalies simultaneously. We obtain that by modifying the definition of a "hit" as defined in item (B.3) to include the requirement that the $\bar{d}$ value for the

coordinated fit to the fictitious mounds be less than or equal to the $\bar{d}$ value for the coordinated fit to the actual mounds. From our ten sets of one million simulations that we ran, we found that on average, for one million simulations, the number of runs that gave 19 or more appearances of these right and isosceles triangles and that had a $\bar{d}$ less than or equal to 3.45 pixels (as in the case of the actual mounds) was about 15.5 ± 2.5. This represents a level of significance of about 0.0000155 and is far less than the common choice of 0.01 used to reject the null hypothesis. Based on this we state that the chances we are in error in rejecting the random geology (or null) hypothesis are extremely remote.

5. Further Tests and Considerations

In this section we describe several additional tests that lend support to the anomalous nature of the mound distribution that we have found.

A. The Four Additional Mounds

Earlier we noted that there are four mounds not taken into consideration, due to their being too tightly clustered in relation to their size, which would allow too great a degree of freedom in making angular measurement. These four mounds are arranged in a square or "cross" pattern, with a hint of another, fifth mound, at the center of this square. The area defined by the four mounds is approximately equal to the average size of the other mounds. Calling this area "mound" S, the analysis was run again for 13 mounds — the original 12, and the area outlined by the four tightly clustered mounds. There is essentially no change in the level of significance.

B. Analysis of Unrelated Right and Isosceles Triangles

The analysis of triangle distributions presented above partners all right triangles (for t from $0°$ to $90°$) with a particular isosceles triangle. A question remains whether there are other favored patterns in the actual mound data involving other pairs of right and isosceles triangles, which unlike our above related right and isosceles, would have no particular relation. Toward this end we have done coordinated fits to right and isosceles triangles defined by $\pi/2$, $(\pi/4 + t/2)$, $(\pi/4 - t/2)$ and $(\pi/2 - t')$, $(\pi/4 + t'/2)$, $(\pi/4 + t'/2)$ with t varying from $0°$ to $90°$ and t' varying *independently* from $-90°$ to $+90°$. Both variations are done in $0.5°$ steps. This includes combinations of pairings of all possible right and isosceles triangles including straight lines (coordinated fits to three mounds lying in a straight line).

We find that the combination with the highest $N(t, t')$ for the actual Cydonia mounds is again at $t = t' = 19.5°$. There are other pairings that are high (above 10) but in all cases they involve either $t = 19°$, $19.5°$, $20°$ and either $t' = 19°$, $19.5°$, $20°$, or $t' = -90°$, $-89.5°$. The latter two angles for the isosceles correspond virtually to straight lines. Thus, the most favored pairings of isosceles and right triangles, besides $t = t' = 19.5°$ involve $t = 19.5°$, corresponding to right

triangles with angles about 35.25°, 54.75°, 90°, and degenerate isosceles triangles with angles of 0°, 0°, 180°.

C. Analysis of Single Triangles with Arbitrary Angles

We next examine the frequency of appearance of arbitrary triangles, including the large class of irregular triangles. Toward this end we have done coordinated fits on the actual mounds to triangles with angles $t, u, \pi - t - u$. We allow t to vary in 0.25° steps from 0° to 60° and allow u to vary from t to 90° $-t/2$ or 90° $- (t + 1)/2$ also in 0.25° steps. We find that there are two different triangles which most frequently appear (12 times). One of them is the ubiquitous right triangles with angles of $\pi/2, (\pi/4 + t/2), (\pi/4 - t/2)$ with $t = 19.5°$, while the other is an obtuse triangle. It is rather startling to find that the angles of that obtuse triangle are given in terms of the same value of t, namely $t, (\pi/4 - t/2)$, $(3\pi/4 - t/2)$ where again $t = 19.5°$. This tendency to favor geometry related to this particular value of t points to an anomaly of geometry as well as one of number and precision. This geometry will be examined more in a future paper.

Another test that could in principle be made would be to consider a fixed set of 1,000,000 randomly chosen 12-mound configurations and one-by-one make a comprehensive search for a striking repetitive or symmetric pattern on each. It could possibly be that a significant subset (*i.e.,* significantly greater in number than the 15.5 we found above) of such configurations would display highly redundant (on the order of 19) patterns of some sort (though very unlikely to be the same pattern for all members of the subset because the search would be comprehensive for each randomly chosen 12-mound configuration). This would not likely diminish the significance of our findings here. The reason is that such a comprehensive study of the actual Cydonia mound configurations would very likely show significantly more striking geometry, certainly more repetitive than that of the 19 related right and isosceles triangles found in this paper. This is seen above where a redundant appearance of another (obtuse), but related triangle is found in the Cydonia configuration. A detailed application of this test will be included of a future paper.

D. An Anomaly of Location

A further mathematical analysis outlined below indicates that the anomalies of number, geometry, and precision are compounded yet again. By using methods of analytic geometry it is possible to show that the configuration of the actual 12 mounds allows a coordinated fit of 11 *prs* and *lrr* triangles with $p = \pi/2$, $r = \pi/4 + t/2$, $s = \pi/4 - t/2$, $l = 2s$ with t in the restricted range from about 18.5° to 20.5° in 0.5° intervals with this number rising sharply to 19 for $t = \arcsin(1/3) = 19.47...°$. At this precise value of the defining angle, the grid location found in our geometrical analysis can be summarized briefly by the following table. It gives the X and Y coordinates of the coordinated fit points of the 12 mounds (and point S at the center of the four small mounds),

transformed and uniformly scaled so that the coordinated fit point of mound G is at the origin and that of mound B at $(X, Y) = (12, -12\sqrt{2})$.

G	A	D	E	B	P	K	J	L	M	O	Q	S
0,0	12,–12	6,–24	0,–12	12,–24	–12,0	4,4	2,4	0,12	6,18	–6,15	–2,4	0,6

This scale is chosen so that all of the coordinated fit points are of the form $(M_i, N_i/\sqrt{2})$ with M and N being integers presented in the table. Applying analytic geometry to the tabulated values of these fit points one can readily show that 12 three mound configurations are *prs* right triangles (EAG, GAD, ABD, EAB, PGE, JPD ,PGL ,GKL, AEL, PLA, MQA, GKO) while 7 three mound configurations are *lrr* isosceles triangles (EAD, PMA, KAE, PEL, QJG, KLQ, GMO) with t = arcsin(1/3). Figure 10 shows that chance is unlikely to be responsible for the 11 appearances on either side of this angle much less the sudden change in N to 19 at this value of the angle. Thus the actual mound placements must be anomalously configured in order for an already rare value of N = 11 to jump to N = 19 for t = arcsin(1/3). This sudden jump from 11 to 19 is a consequence not only of the special proportions of the right and isosceles triangles at that value of t but also the special locations of the actual Cydonia mounds. Without special locations or relative placements of the mounds the number of appearances would be closer to 11 at this angle. A detailed analysis of these claims will be included in a future paper, but to give an example of what we mean consider the effect of adding mound G to the three mound configuration corresponding to the isosceles triangle ADE. Referring to Figure 3 we see that the addition of that one mound adds two right triangles (GEA and GAD). However, these three triangles correspond to two *prs* and one *lrr* triangle with a common value of t *only* for t = arcsin(1/3). For other nearby values of t only one of the two right triangles can be partnered with the isosceles for the same value of t. Here we see how the special proportions of the right and isosceles triangles leads to a jump in the number of appearances from 2 to 3. To see a simple example how a special location can lead to a jump, consider the addition of a fifth mound to the four mound configuration GADE. Mound P clearly would add just one *prs* right triangle. Mound B would also clearly add a *prs* right triangle ABD. However, it also adds a second *prs* right triangle ABE, but only for t = arcsin(1/3). As seen in this simple example, a special position is important in order to take advantage of special proportions.

6. Conclusion

In this paper we have established the existence of an anomaly on Mars in the form of angular placements of relatively small surface features which we call mounds. The anomaly has four aspects: geometry, number, precision, and location. Beginning with the isosceles triad ADE of mounds and continuing through all 12 mounds in the vicinity we have redundant appearances of right and isosceles triangles. Compounding this anomaly is the finding that as we go

from mound to mound the right and isosceles triangles uncovered at the highest frequencies by far in coordinated fits are not independent but are geometrically related to one another. The right triangles we see have proportions that are the same as what you would obtain if you split the isosceles triangle down the middle. Furthermore, this anomaly of number and geometry is accompanied by one of precision. The coordinated fit points are for the most part near the centers of the mounds. Finally, the locations of the mounds are such as to take advantage of a peculiar feature of the geometry (the angle arcsin(1/3)) that defines the proportions of the triangles, increasing the number of appearances of these triangles in a coordinated fit.

We must conclude that the random geology hypothesis fails by a very large margin, that a radical statistical anomaly exists in the distribution of mound formations in this area of Mars. Since previous research in this area seemed to indicate possible anomalies (including, but not limited to, the controversial Face), we had reason to focus on this region. If we had chosen an area at random on Mars and found these mound relations then we should factor in the area of the entire planet in our statistical calculations. But this would presuppose that on average all other regions of Mars had a similar density of mounds and that the only mound anomalies are at Cydonia. Our studies of numerous Viking images shows that mounds of this type in relatively isolated configurations are far from ubiquitous. The existence of this radical statistical anomaly in the distribution of mound formations in this area of Mars indicates in our opinion a need for continued high-priority targeting of the area for active investigation and determination of the origin and nature of the mounds.

Acknowledgments

References

Brownlee, K. A. (1965). *Statistical Theory and Methodology in Science and Engineering.* New York, London, Sydney: John Wiley and Sons, Inc.

Carlotto, M. J. (1988). Digital imagery analysis of unusual martian surface features. *Applied Optics*. 27, 10.

Carlotto, M. J. & Stein, M. C. (1990). A method for searching for artificial objects on planetary surfaces. *Journal of the British Interplanetary Society,* 43, 5.

Carlotto, M. J.(1997). Evidence in support of the hypothesis that certain objects on Mars are artificial in origin. *Journal of Scientific Exploration,* 11, 2.

Carlotto, M. J. (1991, 1997). *The Martian Enigmas: A Closer Look.* Berkeley: North Atlantic Books.

Carr, M. H. (1981). *The Surface of Mars.* New Haven: Yale University Press.

Chandrasekhar, S. (1961). *Hydrodynamic and Hydromagnetic Stability.* Dover: Oxford University Press.

Crater, H. W. (1994). A probabilistic analysis of geomorphological anomalies in the Cydonian region of the Martian surface. Paper delivered in Cody, Wyoming, at the *Moon/Mars conference*.

Crater, H. W. (1995). A statistical study of angular placements of features on Mars. Paper given at *Society for Scientific Exploration* meeting.

Crater, H. W. (1998). Anomalous mound distributions on the Cydonia plain. Poster presentations delivered at the *Spring Meeting of American Geophysical Union,* Boston.

Crater, H. W. (1999). Analysis of land forms on Cydonia Mensa. Poster presentation delivered at the *Spring Meeting of American Geophysical Union,* Boston.

DiPietro, V., Molenaar, G., and Brandenburg, J. (1982, 1988). *Unusual Mars Surface Features*. Mars Research.

DiPietro, V., Molenaar, G., and Brandenburg, J. (1991). The Cydonia hypothesis. *Journal of Scientific Exploration*. 5, 1.

Erjavec, J. & Nicks, R. (1997). *A Geologic/Geomorphic Investigative Approach to Some of the Enigmatic Landforms in Cydonia in The Martian Enigmas: A Closer Look.* Berkeley: North Atlantic Books.

Hoagland, R. C. (1987, 1992). *The Monuments of Mars: A City on the Edge of Forever.* Berkeley: North Atlantic Books.

McDaniel, S. V. (1994). *McDaniel Report: On the Failure of Executive, Congressional, and Scientific Responsibility in Setting Mission Priorities for NASA's Mars Exploration Program.* Berkeley: North Atlantic Books.

O'Leary, B. (1990). Analysis of images of the Face on Mars and possible intelligent origin. *Journal of the British Interplanetary Society,* 43, 5.

Pittendrigh, C. Vishniac, W., and Pearman, J. P. T. Eds. (1964–1965). *Biology and the Exploration of Mars*, Published by National Academy of Sciences National Research Council, Washington DC, 1966. Sagan, C, *et al., Remote Detection of Terrestrial Life,* p. 187–209.

Pozos, R. R. (1986). *The Face on Mars: Evidence for a Lost Civilization?* Berkeley: North Atlantic Books.

Strange, J. F. (1996). Some statistical observations on the distance between some of the mounds at Cydonia. Paper given at the *Society for Scientific Exploration* meeting, Charlottesville, VA.

Stuart, J. T. (1964). On the cellular patterns in thermal convection. *Journal of Fluid Mechanics,* 18, 481.

Suppe, John. (1985). *Principles of Structural Geology.* Edgerton: Prentice Hall.

Torun, E. (1988). *The Geomorphology and Geometry of the D & M Pyramid.* Published electronically on the World Wide Web at: http://www.well.com/user/etorun/pyramid.html.

van Dyke, M., Assembler (1982). *An Album of Fluid Motion.* Stanford: Parabolic Press.